



Influence of graphene functionalization on the curing kinetics, dynamical mechanical properties and morphology of epoxy nanocomposites

Ziani Santana Bandeira de Souza^{a,b} , Pedro Lucas Araújo do Nascimento^b, Mazen Samara^a,
Éric David^a, Guilhermino Jose Macedo Fechine^{c,d} , Maurício Alves da Motta Sobrinho^{a,**},
Nicole Raymonde Demarquette^{a,*}

^a Department of Mechanical Engineering, École de Technologie Supérieure –ÉTS, Montréal, QC, Canada

^b Department of Chemical Engineering, Federal University of Pernambuco – UFPE, Recife, Pernambuco-PE, Brazil

^c School of Engineering, Mackenzie Presbyterian University, São Paulo-SP, Brazil

^d Mackenzie Institute of Research in Graphene and Nanotechnologies - MackGraphe, Mackenzie Presbyterian Institute, São Paulo-SP, Brazil

ARTICLE INFO

Keywords:

Epoxy resin
Curing reaction
Curing kinetics
Functionalization
Graphene
Graphene oxide

ABSTRACT

The properties of graphene have made it a promising material for the development of polymer nanocomposites, and graphene functionalization has gained popularity due to its ability to improve dispersion between the phases. For thermosetting matrices, nanomaterials can affect curing, and rheological studies provide crucial information about this process. This study was undertaken to investigate the impact of graphene functionalization on the curing kinetics and morphology of epoxy nanocomposites. For that, graphene (G), graphene functionalized with surfactant sodium dodecyl sulfate (G-SDS), graphene oxide (GO), and graphene oxide functionalized with amine groups (GON) were used as nanofillers. Rheological studies showed that the addition of graphene to the resin resulted in a slower curing reaction in comparison to the neat epoxy at temperatures of 60 and 70 °C. G-SDS did not affect the curing kinetics of the epoxy resin, while the addition of GO and GON to the resin accelerated the curing kinetics and reduced the reaction activation energy. The most significant improvements were observed for GON, with a reduction in gelation time at 60 °C from approximately 40 min to 17 min, and at 80 °C from 11 min to 6 min, compared to the neat epoxy. The functionalization also resulted in a significant increase in the dynamic storage (E') and loss (E'') moduli, indicating that functionalization of graphene enhances its interfacial interaction with the epoxy matrix. Specifically, GON yielded a 70 % increase in E' and a 28 % increase in E'' compared to the neat epoxy.

1. Introduction

The increasing demand for efficient, lightweight, and cost-effective materials has led to significant interest in polymer nanocomposites. These composites improve the matrix properties by combining it with nanomaterial reinforcements. Even at low filler concentrations, these reinforcements offer enhancements due to their high surface area [1,2]. Epoxy, a widely used thermosetting polymer, possesses excellent adhesion, chemical and thermal resistance, low shrinkage, and strong mechanical properties. Because of these qualities, epoxy is well-suited for high-performance composites in structural adhesives, automotive, aerospace, and coating [3,4].

Graphene is an outstanding option for reinforcing nanocomposites.

Its two-dimensional structure, composed of sp^2 -hybridized carbon atoms, grants graphene a high surface area along with exceptional mechanical, electrical, and thermal properties [5]. Additionally, few-layer graphene (FLG) (comprising 6–10 layers) produced from the exfoliation of natural graphite represents an economical alternative for industrial-scale production [6].

When using graphene to improve the mechanical properties of an epoxy, it is important to ensure that it is well dispersed and evenly distributed throughout the matrix. This is crucial to avoid stress concentration and fractures caused by large agglomerates [7,8]. Therefore, different dispersion strategies have been investigated in the literature [9]. One of the strategies to disperse nanofillers involves modifying their surface by adding different functional groups. These groups are selected

* Corresponding author.

** Corresponding author.

E-mail address: nicoler.demarquette@etsmtl.ca (N.R. Demarquette).

to enhance compatibility between the polymer and the nanofiller by decreasing polar disparity, or forming chemical bonds [10].

The curing reaction is a crucial step in processing thermosetting polymers. It involves mixing a curing agent with the polymer to create a highly cross-linked network by opening the epoxy rings of the monomer. This process transforms the material from a liquid into a solid, resulting in a strong three-dimensional structure. Faster curing systems are essential for improving application efficiency and speeding up production. These systems are important for a variety of uses, including anti-corrosive inner for vessels maintenance [11], adhesives for electronic components [12], and the fabrication of automotive parts [13,14]. Their implementation is vital for enabling high-throughput manufacturing and enhancing overall production efficiency.

Various factors have a significant impact on the kinetics of the nanocomposite cure reaction, such as temperature, functional groups, and dispersion, as well as mobility of the nanomaterials [15,16]. Therefore, it is imperative to investigate the effect of different conditions on the curing time to gain a better understanding of the curing process.

Several studies have used differential scanning calorimetry (DSC) and Fourier-transform infrared spectroscopy (FTIR) techniques to investigate the cure kinetics of graphene/epoxy composites. In addition, various researchers have observed the effects of different nanofillers on the curing process. These studies are summarized in Table 1.

The curing kinetics of a thermoset resin can also be evaluated using rheological measurements [24]. Rheology offers an advantage over other methods by enabling the direct measurement of gelation time, an essential factor in thermoset processing. Beyond this stage, the material transitions into a solid state, making further molding impossible, as the process becomes irreversible. This measurement is accomplished by monitoring the viscoelastic properties of the composite over time while keeping the temperature constant [25]. Despite the importance of this information, the use of rheology to investigate the curing process of

epoxy resins to which graphene has been added is still limited. In this study, rheological tests were employed to examine the curing behavior of epoxy and graphene nanocomposites. To enhance the dispersion between the matrix and the filler, several functionalization methods were used. These include non-covalent functionalization with the surfactant sodium dodecyl sulfate (G-SDS) and covalent functionalization with oxygenated groups (GO) and amine groups (GON). Non-covalent functionalization relies on physical forces of attraction, which is less aggressive and helps preserve the graphene structure. In contrast, covalent functionalization involves chemical reactions. Although this method is more aggressive, the introduction of amine and oxygenated groups can create strong interactions with the epoxy rings in the resin. Therefore, this study aims to investigate the dispersion of various nanofillers in the epoxy resin and their influence on curing kinetics.

2. Methodology

2.1. Materials

Diglycidyl ether of bisphenol A (DGEBA) resin *Epon 828* (Hexion Inc.) and amidoamine curing agent *Epikure 3015* (Hexion Inc.) were purchased from Miller-Stephenson Chemicals.

Few-layer Graphene Black™ 3X was provided by NanoXplore. It can present a carbon content of >91 at.% and approximately 7 at.% oxygen, 0.5 at.% sulfur, and 2 at.% metallic impurities. The average particle size (D50) is 38 µm and the number of layers ranges from 6 to 10. Additionally, powdered graphite (99 % A.P., *Smith*), sulfuric acid (98 % A.P., *Dinâmica*), potassium permanganate (99 % A.P., *Química Nova*), hydrogen peroxide (37 % A.P., *Química Nova*), hydrochloric acid (37 % A.P., *NEON Química*) ethylene glycol (99 % A.P., *NEON Química*), diethylenetriamine (99 % A.P., *Sigma-Aldrich*), ethanol (99 % A.P., *NEON Química*), and dodecyl sulfate sodium (99 % A.P., *Neon Química*) were used.

2.2. Methods

2.2.1. Preparation and characterization of nanomaterials

Graphene, provided by NanoXplore, was functionalized with Sodium dodecyl sulfate surfactant (SDS). For this, a 60 mmol/L SDS solution was prepared and mixed with 10 g of graphene. Then, to remove excess un-adsorbed surfactant, the modified graphene was washed with distilled water and ethanol [26].

Graphite oxide (GrO) was obtained using the modified Hummers' method. First, 1 g of graphite and 25 mL of sulfuric acid were placed in an ice bath at a temperature of 0 °C and stirred for 10 min. Subsequently, 3 g of potassium permanganate were slowly added to avoid sudden increase of temperature. After the addition, the ice bath was removed, and the system was kept at 35 °C for 3 h. To stop the reaction, 150 mL of water and 33 mL of hydrogen peroxide were added, and the material was washed with hydrochloric acid and distilled water to remove impurities [27,28].

To functionalize with amine groups, the aqueous graphite oxide suspension was subjected to an ultrasound bath for 1 h to exfoliate the layers and obtain graphene oxide (GO). Then, 1 g of GO was mixed with 3 g of sodium acetate and 100 mL of ethylene glycol. The mixture was stirred magnetically and heated on a hotplate up to 180 °C. Subsequently, 35 mL of diethylenetriamine was added, and the system was agitated and recirculated for 6 h in a sealed reactor, at 180 °C. Afterwards, the agitation and the heater were turned off, and the content was allowed to cool to room temperature. The material, then, was washed with ethanol and distilled water to remove any unreacted portion [29].

Fig. 1 illustrates the chemical structures of DGEBA (epoxy) and the curing agent, SDS and DETE reagents for functionalization, as well as G, G-SDS, GO, and GON.

Finally, each material underwent a 1-h ultrasonic bath to exfoliate the layers. The Fisher Scientific Ultrasonic Bath 2.8L CPXH Series,

Table 1
Effect of nanofillers on curing reaction.

Filler	wt %	Method	Effect on curing rate	Explanation	Ref.
GNPs	1	DSC	Low T: decrease High T: increase	Low T: steric hindrance effect High T: high thermal conductivity of GNPs reduced the steric hindrance effect.	[17]
GO	0.5	DSC	Increase	Oxygenated groups can react with resin epoxy ring	[18]
GO	0.1	DSC	Decrease	Steric hindrance effect	[19]
GrO	0.5	DSC	Decrease	Oxygenated groups can react with curing agent	[20]
GO	1	DSC	Decrease	Oxygenated groups can react with curing agent	[21]
GO	2	DSC FTIR	-	Oxygenated groups can react with curing agent	[22]
GO-DETE GO-PEHE	0.1	DSC	Increase	High dispersion, reaction with resin epoxy ring	[19]
pDop-rGO	0.5	DSC	Increase	High dispersion, reaction with resin epoxy ring	[23]
GO - hexamethylene diamine	1	DSC	Increase	High dispersion, reaction with resin epoxy ring	[21]
GrO -poly (oxypropylene) diamine	0.5	DSC	Decrease	Increment of viscosity and steric hindrance effect	[20]

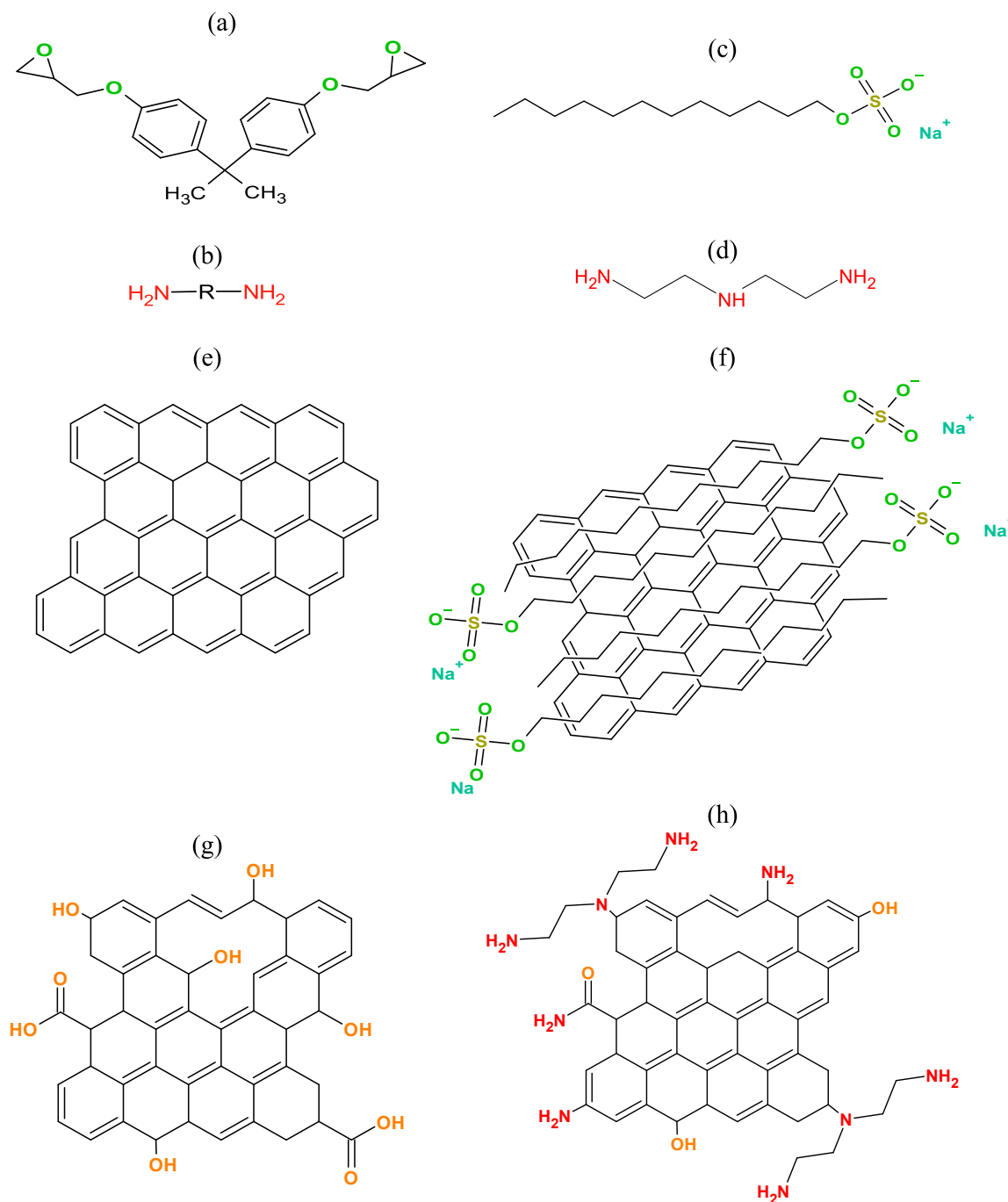


Fig. 1. Schematic representation of (a) DGEBA, (b) curing agent, (c) SDS, (d) DETE, (e) G, (f) G-SDS, (g) GO and (h) GON.

operating at 40 kHz and room temperature, was used for this process.

The nanomaterials were characterized via X-ray photoelectron spectroscopy (XPS), thermogravimetric analysis (TGA), Raman spectroscopy, X-ray diffraction (XRD), and scanning electron microscopy (SEM). Before conducting the tests, the samples were dried in a vacuum oven for 24 h. The XPS analysis was performed on a VG ESCALAB 250Xi, equipped with a Mono Al $K\alpha$ source and a 1486.68 eV pass energy. The *Advantage v6.5* software was used to analyze the spectra. This involved fitting all high-resolution peak components using symmetrical Lorentzian/Gaussian peak functions, except for the C1s peak component related to sp^2 graphitic carbon, which is asymmetrical. To ensure consistent results of carbon-oxygen, nitrogen, sodium, and sulfate species, asymmetry parameters were optimized from C1s, O1, N1s, Na1s

and S2p. TGA was performed using a PerkinElmer Pyris Diamond TGA/DTA in N_2 atmosphere. Approximately 10 mg of the sample was placed in an aluminum pan. The analysis was carried out at a heating rate of $10\text{ }^\circ\text{C}\cdot\text{min}^{-1}$ over a temperature range of 40–600 $^\circ\text{C}$. Raman spectroscopy was performed using a confocal Raman spectrometer WITec UHTS 300. The samples were analyzed in several locations by a laser excitation source with a wavelength of 532 nm and a power of 1.5 mw. The data were analyzed using the *WITEC Project* software. The XRD method was performed using a XRD diffractometer X'Pert³ Panalytical with a copper monochromator ($CuK\alpha = 1.54\text{ \AA}$). Values of 2θ between 3.5° and 70° were used, with $\Delta 2\theta = 0.01$, a voltage of 45 kV and a current of 40 mA. The SEM was performed in a scanning electron microscope Hitachi TM 3000, at an accelerating voltage of 15 kV.

2.2.2. Preparation of composites

The nanocomposites were prepared using the solution mixing method. The DGEBA and the nanomaterial in the aqueous solution were mixed by magnetic stirring. The system was maintained at 60 °C for 15 h to allow water to evaporate, which was confirmed by thermogravimetric analysis (TGA). Finally, the curing agent was added and manually stirred for 1 min. The weight ratio of the nanomaterial, DGEBA, and curing agent was 1 : 68.3: 30.7, respectively.

After preparation, the mixture was placed in a vacuum oven at 40 °C for 15 min for degassing. Finally, the samples were promptly transferred to the rheometer for kinetic testing. Additionally, specimens were prepared by pouring the mixture into molds, which were then placed in an oven at 80 °C for 3 h until fully cured, in accordance with the manufacturer's specifications.

2.2.3. Composites characterization

a) Rheological analyses

To investigate the cure kinetics, samples of the neat epoxy (E) and epoxy composites reinforced with graphene (G/E), graphene-SDS (G-SDS/E), graphene oxide (GO/E) and graphene oxide functionalized with amine groups (GON/E) were prepared right before the testing. The cure of these materials was investigated using a rotational rheometer. For that, the materials were subjected to small amplitude oscillatory shear at a constant amplitude, frequency and temperature, in the linear viscoelastic regime previously determined. This method allows for verifying the flow properties of the materials as a function of time.

The rheological test allows also determining the gelation time, which corresponds to the liquid-rubber transition and is an irreversible process [30]. In the literature, the gelation time has been identified through oscillatory rheological testing using different criteria. Most studies determine the gel point by identifying the crossover of G' and G'' , marking the transition from liquid-like to solid-like behavior in the material [31,32] for one experiment performed at one frequency. Although straightforward and widely used, this method can suffer from inaccuracy as the result will depend on the frequency (ω) of the applied oscillation. An alternative criterion, proposed by Winter–Chambon, defines the gel time as the point at which G' and G'' exhibit the same scaling law [33,34]. Consequently, the gel point, which is a frequency-independent phenomenon, is indicated as the intersection point of the loss factors obtained at different frequencies [34–36]. More details about the justification for the use of this lengthier method can be found in the original manuscript. Within the present work, the Winter–Chambon criterion was utilized.

Tests were carried out using an Anton Paar Physica MCR 501 rheometer with a disposable parallel plate geometry. This setup included a disposable upper plate with a diameter of 25 mm and a lower disposable fixed plate with a diameter of 50 mm. Time sweep tests were performed using a strain amplitude of 2 % and angular frequencies of 10, 20 30 and 40 rad/s. These tests were carried out at constant temperatures of 60 °C, 70 °C, and 80 °C and 1.5 mL of the sample was used in each test.

Using the data of gelation time as a function of temperature, it was possible to evaluate the activation energy for the curing reaction. This was achieved using the kinetic model for the curing process combined with the Arrhenius equation, according to Equation (1) [37].

$$\ln(t_{gel}) = c + \frac{E_a}{R} \frac{1}{T} \quad (1)$$

Where t_{gel} is the gelation time, E_a is the activation energy, R is the gas constant, and T is the temperature, and c is a constant.

b) Chemical analyses

In order to identify the functional groups formed during the curing reaction, an investigation was conducted on the epoxy and its composite samples using Fourier-transform infrared spectroscopy (FTIR) at different intervals during the curing process at 60 °C. The samples were subjected to controlled conditions, being placed in an oven at 60 °C, removed after specified intervals, and frozen for subsequent characterization. The analyses were carried out utilizing a PerkinElmer Spectrum 100 FTIR spectrometer coupled with an Attenuated Total Reflectance (ATR) crystal, with speed of 10 kHz, and a temperature and humidity below 21 °C and 60 %, respectively.

The degree of conversion of the epoxy rings (α) for the epoxy and its composites was calculated using the area under the peak at wavenumber 915 cm^{-1} (A_{915}), normalized by the area under the peak at wavenumber 1608 cm^{-1} as a reference (A_{1608}), at different times (t), according to Equation (2) [38].

$$\alpha = 1 - \frac{(A_{915} / A_{1608})_t}{(A_{915} / A_{1608})_0} \quad (2)$$

c) Mechanical analyses

Dynamical mechanical analysis (DMA) was used to evaluate the mechanical properties of the composite and indirectly exam the interfacial interaction between filler and matrix. The test was carried out on using an Anton Paar MCR 702 rheometer equipped with a three-point bending linear device. The test specimens were fully cured in oven at 100 °C for 2h, and had dimensions of 70 mm (length) \times 10 mm (width) \times 4 mm (thickness). Measurements were carried out from 25 °C to 175 °C at a heating rate of 5 °C/min, a frequency of 1 Hz and a strain of 0.1 %.

The morphology of the composites was investigated by scanning electron microscopy (SEM). The specimens were cryogenically fractured in liquid nitrogen and sputter coated with a thin layer of platinum. Then, they were analyzed in a field emission gun scanning electron microscope Hitachi SU 8230, at an accelerating voltage of 5 kV.

Optical microscopy was also employed to investigate the samples of epoxy and its composites before the curing process. The analysis was performed using an Olympus BX51 Fluorescence Microscope. For that, a drop of the material was placed between two microscope slides to form a thin layer.

3. Results

3.1. Nanomaterials characterization

The composition of modified graphene was analyzed using X-ray photoelectron spectroscopy (XPS). High-resolution spectra of C1s, O1s, N1s, Na1s, and S2p3 are shown in Fig. 2, while Table S1 displays the compositions of each group present.

The C1s spectrum of graphene oxide revealed peaks centered at 289.2, 287.8, 287, 285.2, and 284.5 eV, which correspond respectively to the ester and carboxyl (O=C–O), carbonyl (C=O), hydroxyl (C–OH) groups, C–C resulting from sp^3 hybridization and C=C resulting from sp^2 hybridization [39]. The O1s spectrum also confirmed the presence of oxygenated groups, with peaks centered at 532, 532.8, and 533.6 eV, corresponding to C=O or O=C–O bonds and the C–OH group [40].

Graphene oxide comprises carbon in the sp^2 hybridization (C=C–C) and carbon in the sp^3 hybridization (C–C), indicating that the functionalization of graphite with oxygenated groups leads to a modification of the hybridization of the carbons present in the basal plane. With the amino functionalization of graphene oxide, significant changes in the spectra were observed. Compared to GO, GON showed an increase in sp^3 hybridization carbons, confirming the higher level of disorder in the structure due to functionalization. A contribution at 285.9 eV in the C1s spectrum of GON is attributed to the C–N bond [41]. Moreover, the

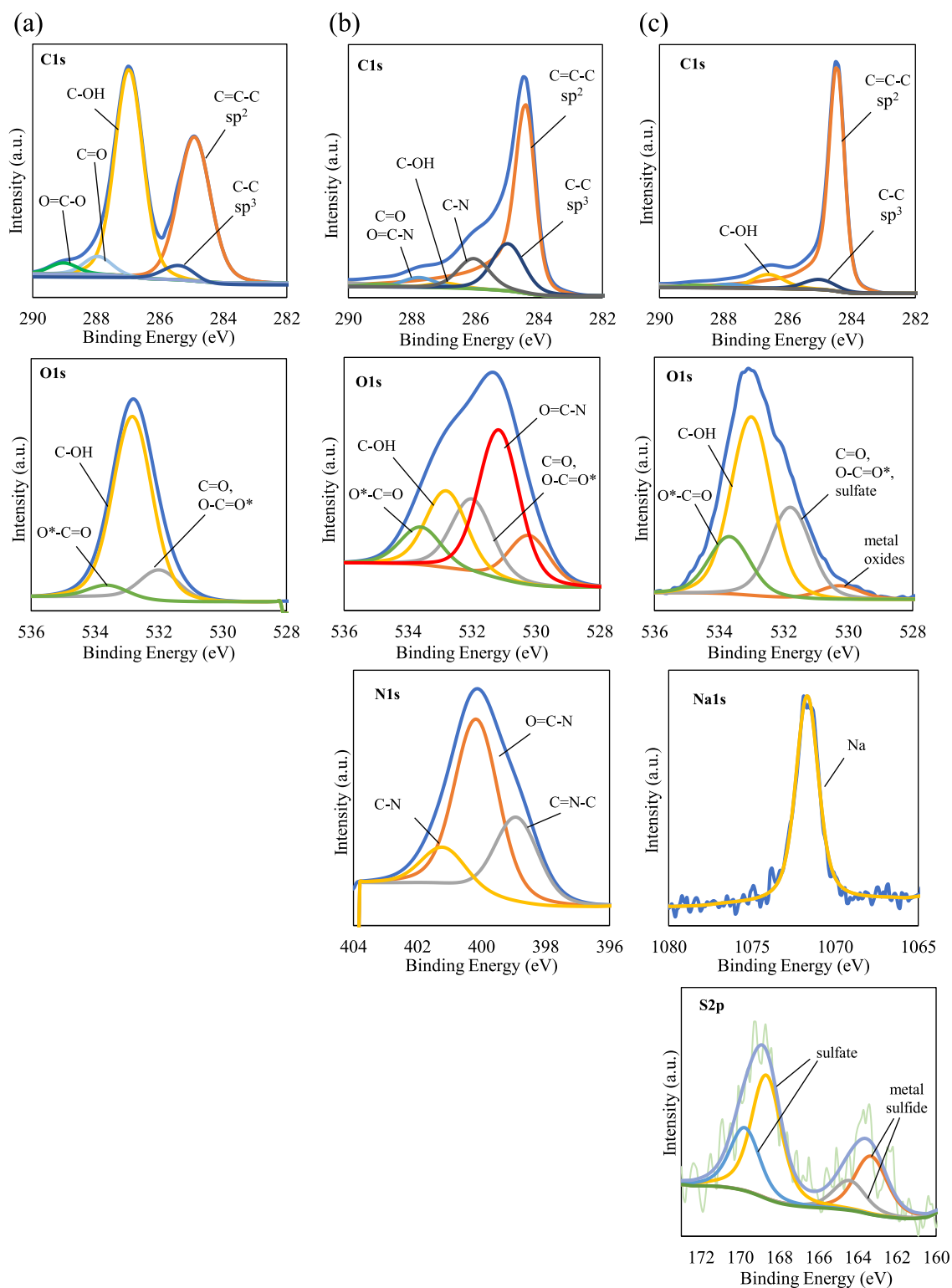


Fig. 2. High resolution center-level XPS spectra C1s, O1s, N1s, S2p and Na1s of GO (a), GO-N (b) and G-SDS (c).

peaks at 398.4 and 399.7 eV on N1s spectrum confirmed the presence of amine groups.

For G-SDS, a peak was observed at 1071.7 eV in the Na1s spectrum, and another peak at 168.7 eV in the S2p spectrum, corresponding to sodium and sulfate from the addition of the surfactant. Moreover, it showed a small percentage of oxygenated groups and a higher content of carbon in sp^2 hybridization, indicating that most of the structure of graphene has not undergone major alterations.

TGA shown in Fig. 3 demonstrates different thermal characteristics of the nanomaterials. Considering that XPS is a surface analysis technique, TGA can provide insight into the functionalization content of the entire bulk sample, as it evaluates changes in weight related to the degradation of functional groups throughout the material. Graphene displayed a slight weight loss of 1.59 %, mainly attributed to moisture, leftover oxygenated groups, or impurities. G-SDS, in contrast, showed a 10 % weight loss in the temperature range of 250–300 °C due to

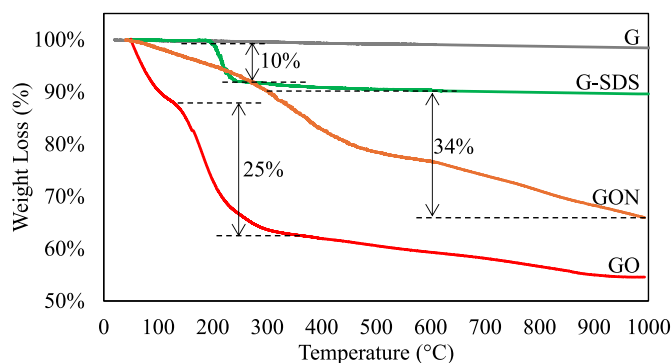


Fig. 3. TGA curves of G, G-SDS, GO, and GON.

surfactant degradation, which reflects the weight content of the functionalization on the graphene surface [42]. For the GO, two major weight loss ranges were observed: a 12 % loss between 30 and 130 °C due to moisture removal, and a 25 % loss between 150 and 350 °C linked to the degradation of oxygenated groups. This 25 % loss reflects the oxidation level of graphene oxide [43]. Above 350 °C, a mild additional loss occurred, resulting in a total weight loss of 53 %. GON displayed a weight loss of 2.8 % between 30 and 130 °C. In the 150–350 °C range, a lower weight loss of 10 % was observed, and the reduction in comparison of the GO is linked to the partial reduction of oxygenated groups due to the functionalization process. A gradual loss above 300 °C was attributed to the degradation of nitrogen groups, with a total weight loss of 34 %, which corresponds to the level of functionalization of GON with amine groups [44].

The complementary characterization of nanomaterials (XRD, Raman spectroscopy and SEM) is provided in the supplementary material (Figs. S1 and S2).

3.2. Curing kinetics

Fig. 4 presents a typical time sweep behavior for the samples studied in this work. In this case it is shown the storage and loss moduli for the epoxy and its composites, subjected to time sweep at a frequency of 10 rad/s, and a temperature of 60 °C. Similar behavior was observed for all the samples studied here for every frequency. Initially, the loss modulus (G'') was higher than the storage modulus (G') because the mixture was in the liquid state and the mobility of the molecules was high. As the

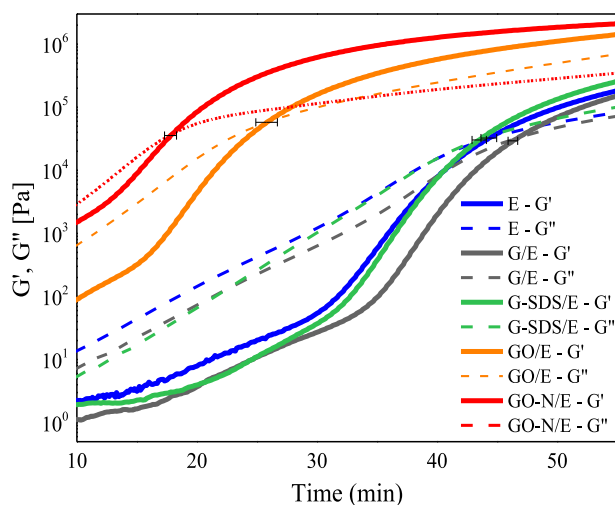


Fig. 4. Evolution of storage and loss moduli for epoxy resin and composites (G/E, G-SDS/E, GO/E, GO/N) at 60 °C. Conditions: frequency = 10 rad/s, amplitude = 0.2 %, LVR.

curing reaction proceeded, cross-links were formed between the polymer chains, which restricted their movement. Consequently, the storage modulus increased significantly, surpassing the loss modulus.

• Gelation Time

Fig. 5 shows the time sweep of the epoxy and the composite graphene oxide amine functionalized/epoxy at the different frequencies tested in this work. The plots display the storage modulus (G'), loss modulus (G''), and $\tan \delta$ as functions of time. The Winter-Chambon criterion was applied in this work to determine the gel point, which defines the gel point as the moment when $\tan \delta$ becomes independent of frequency. The gelation time values are summarized in Table 2.

For the test conducted at 60 °C, the neat epoxy resin exhibited a gelation time of 40.5 min (± 0.6). The addition of graphene resulted in a slightly increased gelation time of 44.2 min (± 0.4), indicating a minor retardation effect caused by the graphene. Due to its non-polar nature, graphene tends to disperse poorly in the epoxy matrix and consequently form more agglomerates. The agglomerates can act as a physical barrier and prevent the polymer chains from forming a three-dimensional network [45]. As the temperature increased to 70 °C, similar behavior was observed. At a temperature of 80 °C, it was noticed that the graphene gelation time was the same as that of the pure polymer. This means that the steric effect of graphene was reduced because the polymer chains had greater mobility at higher temperatures.

With the addition of G-SDS, there were only minor differences in gelation time compared to the neat epoxy. The surfactant may have improved material dispersion, eliminating steric effects of graphene.

By adding GO and GON, there was a significant reduction in reaction times, especially for GON. The hydroxyl and carbonyl groups in GO may have reacted with epoxy groups present in the resin. Similarly, amine groups are also capable of triggering epoxy resin ring-opening reactions. Furthermore, the longer chain length of DETA may facilitate the reaction by further reducing the gelation time.

• Activation Energy

The activation energy was calculated as the slope of the plot of $\ln(t_{gel})$ vs. $1/T$, since R is a constant. The results are presented in Fig. 6. The activation energy supported the observed gel time trend. It was found that the presence of graphene increased the activation energy compared to pure epoxy, indicating that the filler acts as a barrier that hinders the reaction. Additionally, the functionalization with surfactant reduced the steric effect and lowered the activation energy. The analysis also revealed a significant decrease in the curing reaction's activation energy with the use of GO and GON. Thus, it can be concluded that these materials facilitated the reaction [46].

• Chemical analyses

Fig. 7 shows the FTIR spectra for neat epoxy (Epon 828 DGEBA/Epikure 3015 system curing agent) at different times after the addition of the curing agent for an experiment carried out at 60 °C. The characteristic peaks are described in Table 3. Among the peaks, the following are particularly noteworthy: a broad band at 3350 cm^{-1} , attributed to the O–H stretching of hydroxyl groups; a peak at 1608 cm^{-1} , related to the C=C stretching of aromatic rings; and a peak at 915 cm^{-1} , associated with the C–O stretching of epoxy groups. Since the curing agent is composed of amidoamine, peaks related to nitrogen-containing groups can also be observed [47–49]. The peak at wavenumber 1608 is widely used as a reference peak [38], as aromatic rings are chemically more stable and do not participate in the curing reaction. Thus, the obtained curves were normalized by the transmittance of this peak.

As seen in Fig. 7, with the increase in curing time, there was a reduction in the peak at 915 cm^{-1} , indicating that the epoxy group is being consumed. Due to its cyclic configuration, the epoxy group is

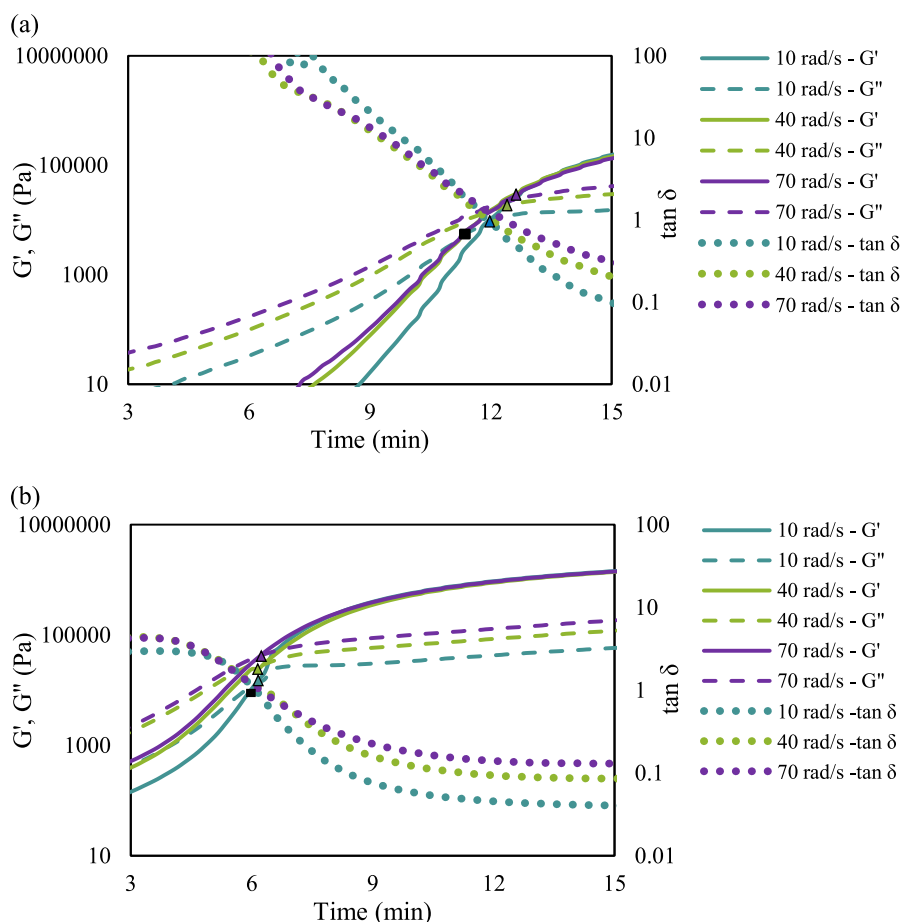


Fig. 5. Determination of the gelation time at 80 °C, amplitude = 0.2 % for E (a) and GON/E (b): crossover of storage and loss moduli (marked by triangles) and the point where $\tan \delta$ is frequency-independent (indicated by squares).

Table 2

Gelation time of the epoxy resin and its composites.

Material	Gelation time (min) (\pm standard deviation)		
	60 °C	70 °C	80 °C
E	40.5 (\pm 0.6)	21.5 (\pm 0.2)	11.2 (\pm 0.7)
G/E	44.2 (\pm 0.4)	23.5 (\pm 0.6)	11.5 (\pm 0.7)
G-SDS/E	35.5 (\pm 0.6)	18.5 (\pm 0.5)	10.5 (\pm 0.8)
GO/E	26.0 (\pm 0.8)	16.2 (\pm 0.8)	8.50 (\pm 0.7)
GON/E	17.0 (\pm 0.4)	10.5 (\pm 0.6)	6.17 (\pm 0.6)

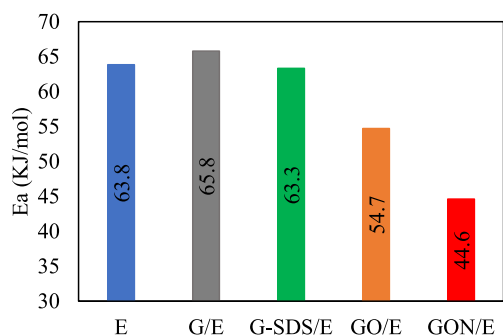


Fig. 6. Activation Energy of the epoxy and its composites.

highly reactive and susceptible to nucleophilic attack via an S_N2 nucleophilic addition reaction. In this reaction, the proton is transferred from the nucleophile to the epoxy group, resulting in ring opening. The primary and secondary amines of the curing agent are capable of reacting with the epoxy groups, resulting in the formation of a tertiary amine and a hydroxyl group. This was confirmed by the increase in the broad band at 3350 cm^{-1} . The schematics of those reactions are presented in Fig. 8a-b. Additionally, an increase in the peak at 1036 cm^{-1} over time was observed, which is associated with the ether group. This indicates that homopolymerization is occurring, as the epoxy group reacts with the hydroxyl group, as illustrated in the schematic in Fig. 8c [50,51].

The FTIR spectra for the different composites exhibited similar behavior as the neat epoxy, as can be seeing in Fig. 7b. In the case of GO, XPS analysis confirmed the presence of carboxyl and hydroxyl groups. These groups are nucleophilic and react with the epoxy ring to form ether and ester groups (Fig. 8a-b). Additionally, GON contains primary and secondary amine groups, as well as the oxygenated groups that were not fully reduced during functionalization. Therefore, the reaction with the epoxy ring can occur via four different pathways (Fig. 8a-d). Finally, for the G-SDS/E spectrum (Fig. 7b), no new peaks were added, indicating that the presence of sulfhydryl groups did not contribute to the epoxy ring opening reaction.

The degree of conversion (α) for epoxy and its nanocomposites are shown in Fig. 9. At equivalent reaction times, G/E exhibited lower conversion rates compared to neat epoxy, reaching the maximum degree of conversion more slowly. In contrast, G-SDS/E displayed conversion rates nearly identical to neat epoxy, while GO/E and GON/E

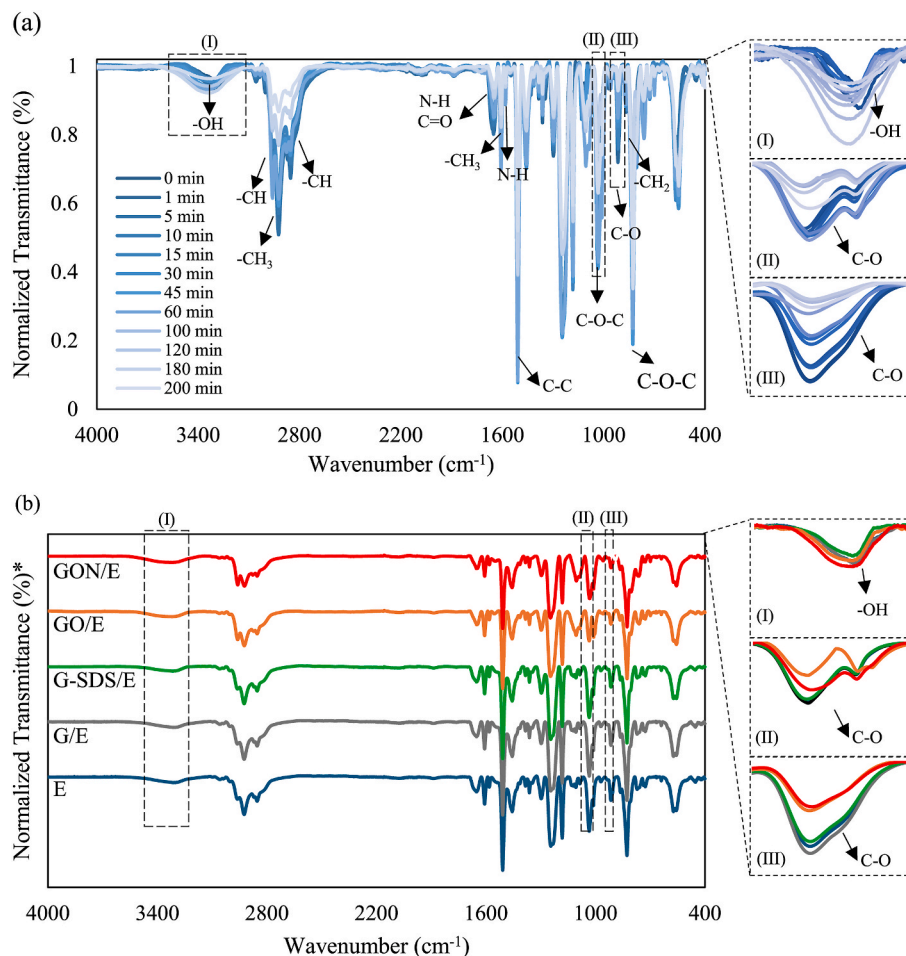


Fig. 7. FTIR spectra during the isothermal curing at 60 °C: (a) epoxy at different curing times; (b) epoxy and its composites 15 min after curing started (*curves offset along the y-axis for clarity).

Table 3

Characteristic bands of DGEBA and curing agent.

Contribution	Wavenumber (cm ⁻¹)	Functional group	Vibration type
DGEBA	3350	O-H	Stretching of hydroxyl groups
	3050	C-H	stretching of the oxirane ring
	2970–2873	C-H	stretching of CH ₂ and CH aromatic and aliphatic
	1608	C=C	stretching of the aromatic rings
	1505	C-C	stretching of aromatic
	1384	-CH ₃	symmetric deformation of the carbon chain
	1036	C-O-C	stretching of the ether group
	915	C-O	stretching of the oxirane group
	830	C-O-C	stretching of the oxirane group
	772	CH ₂	rocking
Amidoamine curing agent	1582	N-H	stretching of the secondary amine group
	1657	N-H, C=O	stretching of the secondary amides
	1122	C-N	bond stretching

demonstrated higher conversion rates, achieving 100 % conversion more rapidly under the same conditions. Those results align with the rheological results at 60 °C, highlighting the accelerating effect of the GO and GON.

3.2.1. Dynamic mechanical analysis

Fig. 10 shows the variations in storage modulus (E') and loss modulus (E'') with temperature for the epoxy and its nanocomposites. The values of E' , E'' and T_g are reported in Table 4.

All nanocomposites showed increases in E' , which can be attributed to two factors: (1) the higher modulus of the fillers compared to epoxy, and (2) the creation of a filler-matrix interface, which contributes to the dissipation of external stresses and results in a reinforcing effect. Thus, the more significant increase for G-SDS/E compared to G/E indicates that this functionalization enhanced the interface between the matrix and the filler [52].

This increase in E' was even more pronounced for GO/E and GON/E, with E' increasing by 60 % and 70 %, respectively. This occurs due to the functional groups present in the nanomaterials, which can react covalently with the epoxy resin, thereby restricting the mobility of the polymer chains. Furthermore, the greater compatibility of epoxy with the amine groups of GON enhances dispersion within the matrix, resulting in a more significant restrictive effect [53,54] as can be seen Fig. 11, which shows a comparison of the morphologies of the different composites studied in this work. In the literature, studies on the functionalization of graphene with amine groups have also reported enhancements in the E' compared to neat epoxy, with improvements of approximately 17 % [55], 22 % [56], and 25 % [57], for samples

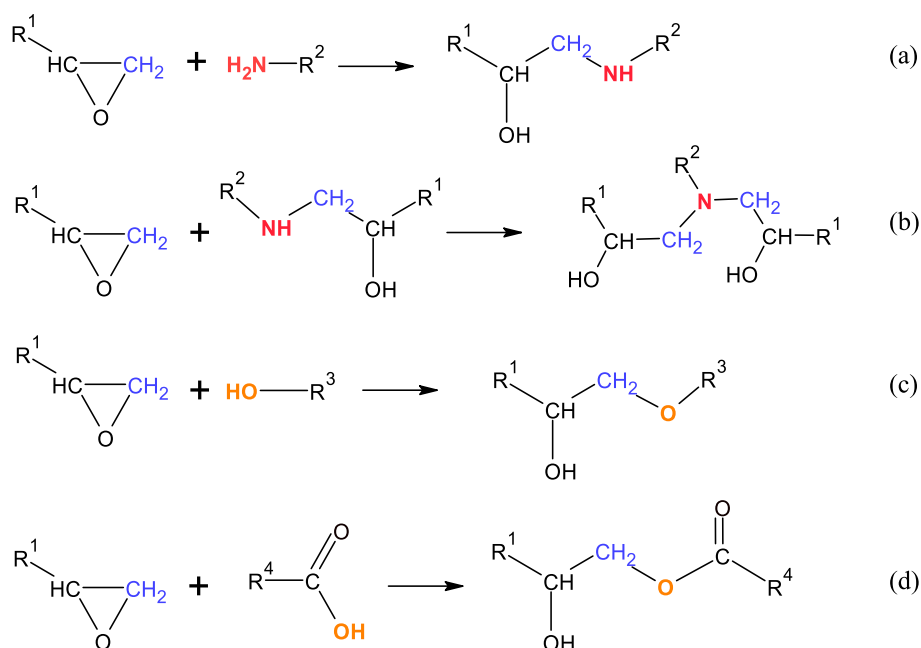


Fig. 8. – Schematics of epoxy group reactions with primary amine (a), secondary amine (b), hydroxyl group (c), and carboxyl group (d).

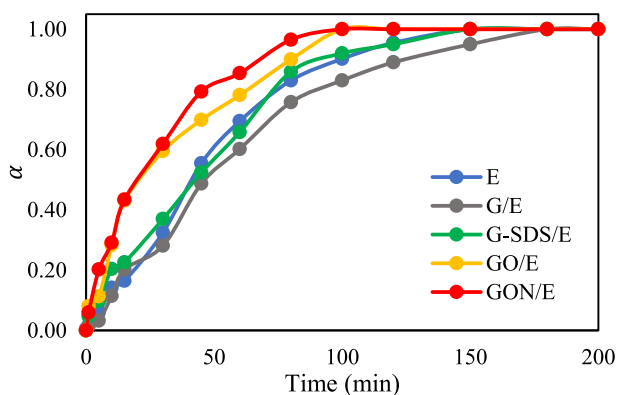


Fig. 9. Degree of conversion of epoxy rings for the epoxy and its composites at different times during isothermal curing at 60 °C.

containing 1.03 vol%, 1 wt%, and 0.125 wt% amine-functionalized graphene, respectively.

An increase in E'' and a peak shift were also observed, especially for the GO/E and GON/E. This behavior indicates that the system has

become more flexible, due to the greater tendency to dissipate energy. The peak temperature of E'' is also used to obtain T_g . As a result, there was an increase in T_g for the GO and GON reinforcements, indicating an increase in the crosslink density of the epoxy matrix [58].

The Optical Microscopy (MO) analysis (Fig. 12) confirmed the findings from the scanning electron microscopy (SEM) observations. The G/E samples exhibited larger agglomerates, while the G-SDS/E samples showed a slight reduced agglomerate sizes. In contrast, the GO/E and GON/E samples displayed a more uniform dispersion that nearly covered the entire epoxy region, with only a few isolated areas of pure epoxy and some larger agglomerates present.

Table 4

Dynamic mechanical properties of epoxy and composites.

Material	E' (MPa)	E'' (MPa)	T_g (°C)	E' increase (%)	E'' increase (%)
E	1125.6	196.4	58.29	–	–
G/E	1327.4	213.1	59	+18 %	+9 %
G-SDS/E	1450.2	224.2	59.23	+29 %	+14 %
GO/E	1785.0	237.5	63.57	+60 %	+21 %
GON/E	1917.2	252.0	75.51	+70 %	+28 %

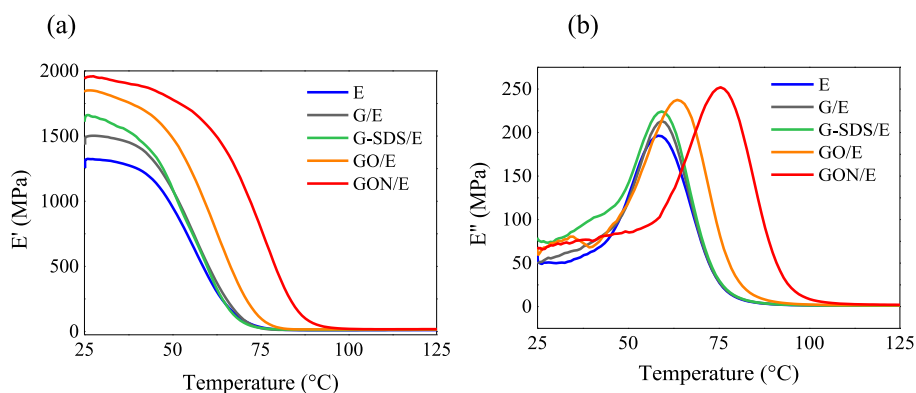


Fig. 10. Dynamic mechanical properties curves of the epoxy and its composites.

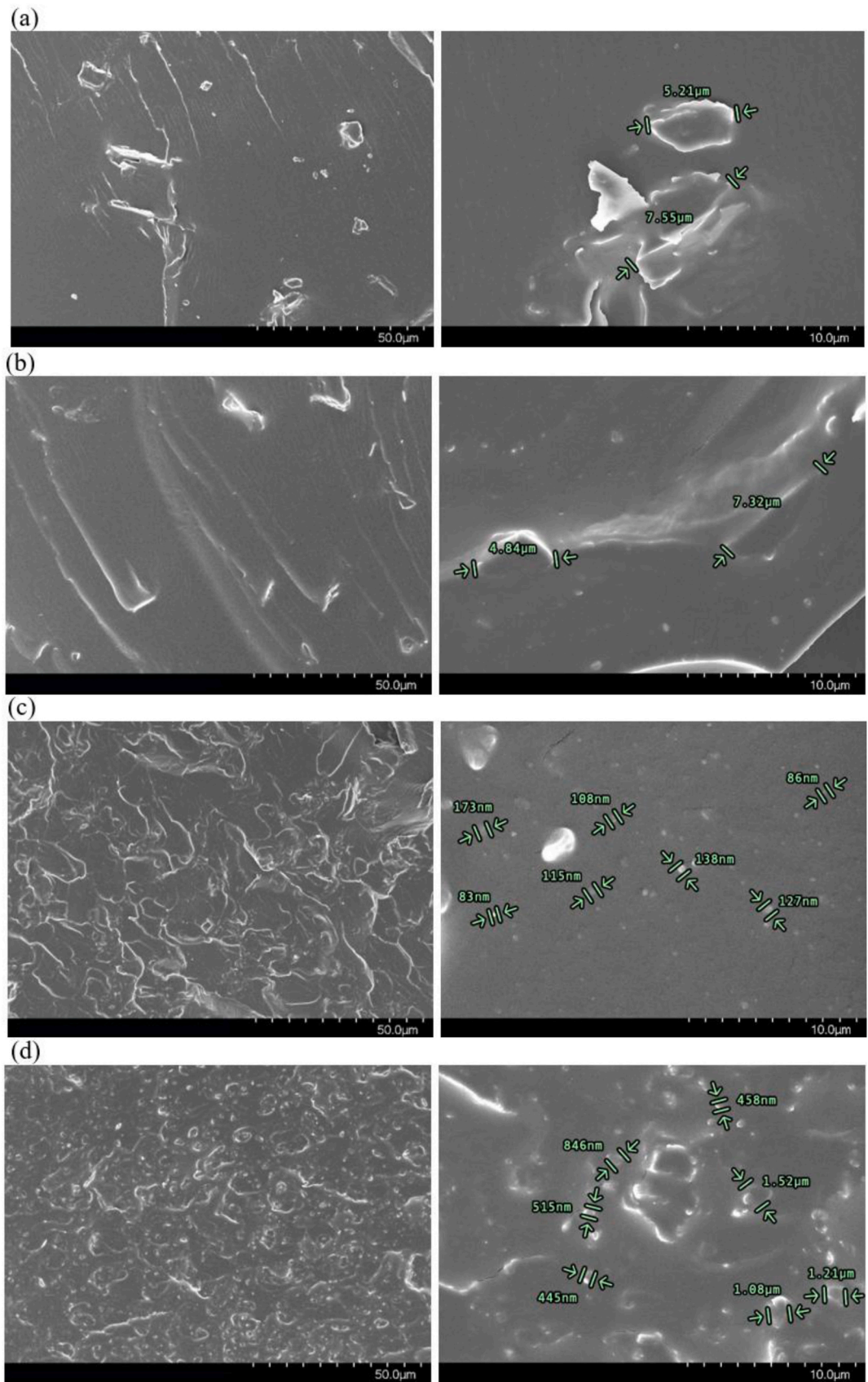


Fig. 11. SEM micrographs of G/E (a), G-SDS/E (b), GO/E (c), and GON/E (d) composites at scale of 50 μm and 10 μm.

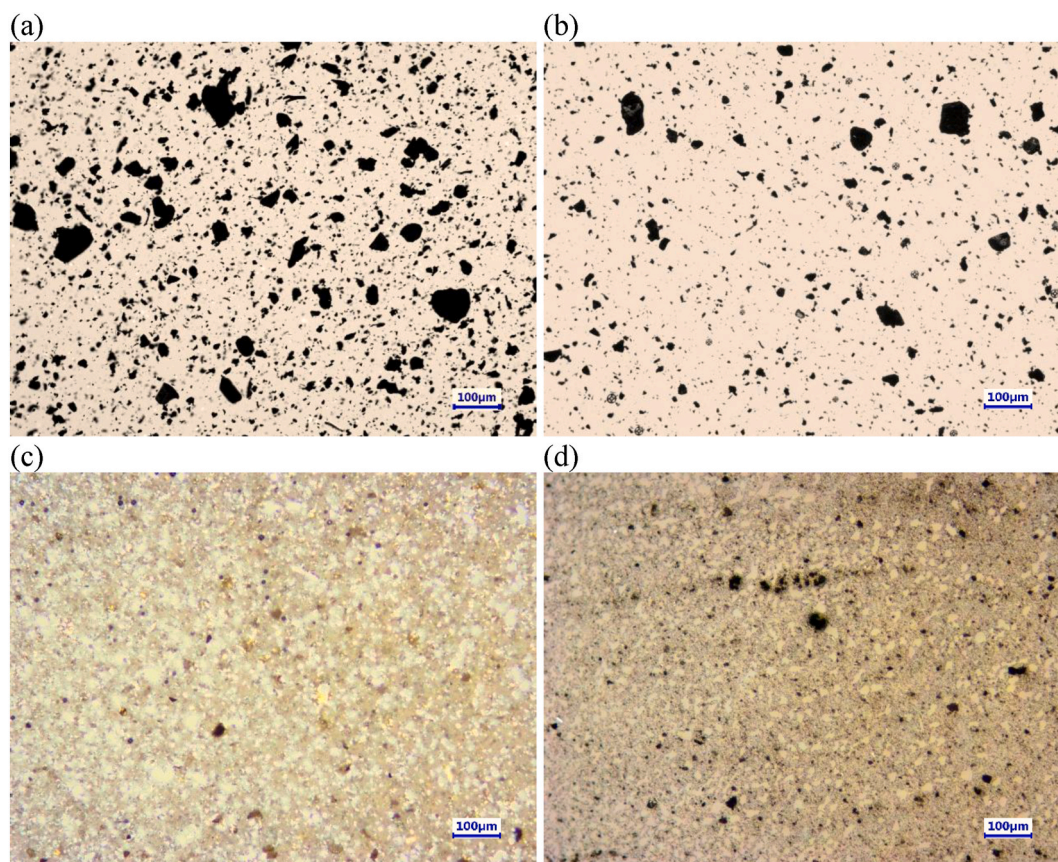


Fig. 12. Optical microscopy images of G/E (a), G-SDS/E (b), GO/E (c) and GON/E (d) composites.

4. Discussion

Rheological tests indicate that when graphene was added to the epoxy at low temperatures, the steric effect was predominant due to the larger cluster sizes observed via SEM, as depicted in Fig. 13a. Consequently, as observed by FTIR, G/E exhibited a lower conversion of the epoxy rings compared to neat epoxy. However, this effect diminished at 80 °C due to increased chain mobility. A similar temperature-dependent

behavior was observed by S. Rehman et al. [17].

The presence of the surfactant was found to suppress the steric effect at all temperatures, indicating improved dispersion, as shown in Fig. 13b. Although the SEM micrograph did not show significant differences in agglomeration size between G/E and G-SDS/E, further DMA analysis showed an increase in E' , associated with strong interactions between the functional groups and the matrix, enabling more efficient load transfer.

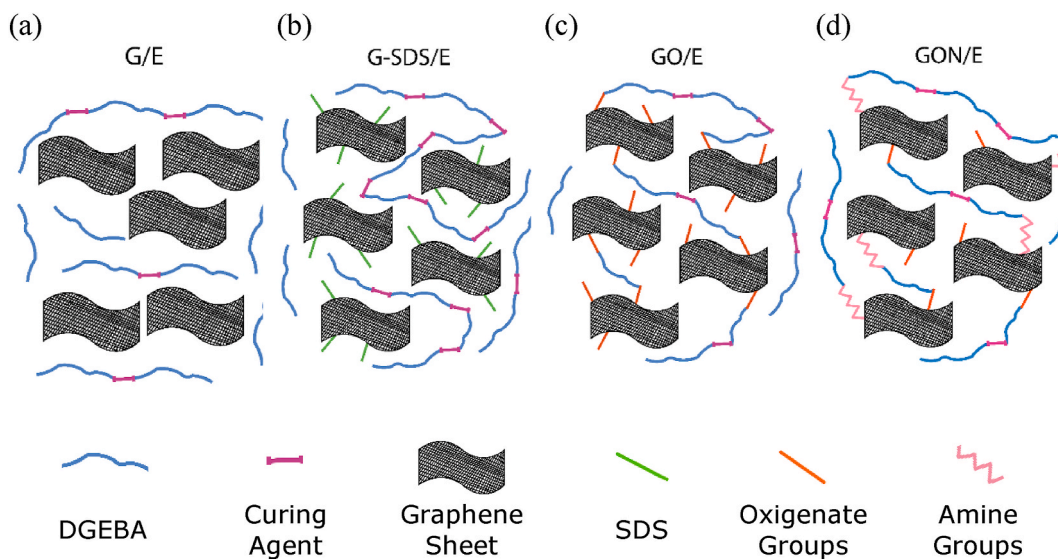


Fig. 13. Schematic representation of the curing of composites (a) graphene/epoxy at low temperature, (b) graphene-SDS/epoxy, (c) graphene oxide/epoxy and (d) graphene oxide functionalized with amine groups/epoxy.

For graphene oxide, different studies report both an accelerating effect [18] and an inhibitory effect [21]. In our study, functionalizing graphene with oxygenated and amine groups led to a reduction in gelation time and an increase in epoxy group conversion. These functionalizations introduce proton donors such as alcohols, carboxylic acids, and amine groups. The presence of hydroxyl and carbonyl groups in GO and amine groups in GON facilitates epoxy ring-opening reactions, as shown in the schematics in Fig. 8, thereby accelerating the curing process. This effect was more pronounced for GON due to the longer chain length of DETA, which likely enhanced the reaction rate, as shown in the schematic in Fig. 13c,d.

Moreover, the changes observed for the addition of GO and GON were obtained by the addition of 1 wt% of these nanomaterials, equivalent to around 0.35 wt% of functional groups, according to XPS and TGA. This amount is small compared to the combined mass of DGEBA and curing agent (68.3 wt% and 30.7 wt%). It suggests that the added portion has minimal impact on the reaction's stoichiometry, indicating that the nanomaterials might have acted as heterogeneous catalysts by providing active surfaces that facilitate the chemical reaction.

5. Conclusion

The present study demonstrated that the functionalization technique used for graphene reinforcement can significantly impact the curing of epoxy composites. Graphene, graphene functionalized with SDS, graphene oxide, and amino-functionalized graphene oxide were evaluated as fillers for the epoxy matrix. To achieve this, isothermal rheological tests in the oscillatory regime were conducted to assess the viscoelastic properties of the material over time. Additionally, the evolution of the chemical structures of the epoxy as a function of time was also evaluated by FTIR.

By examining the rheological and FTIR results, it was found that the addition of graphene resulted in a delay of curing at lower temperatures due to the steric hindrance, but this effect disappeared at higher temperatures, due to the higher mobility of the polymer's chains. G-SDS didn't interfere in the curing reaction in all studied temperatures, indicating the surfactant helped to enhance the dispersion and reduce the hindrance effect. Concomitantly, GO and GON accelerated curing and reduced activation energy, since the functional groups were able to form covalent bonds with the epoxy resin. Moreover, the microscopy images and the improvements in the mechanical dynamical properties showed that GO and GON were efficient in improving the dispersion. Thus, functionalized graphene enhances curing efficiency, which is vital for reducing processing times, increasing production capacity, and streamlining maintenance processes. This makes it valuable for industrial applications that require rapid curing and high-performance materials.

CRedit authorship contribution statement

Ziani Santana Bandeira de Souza: Writing – original draft, Validation, Methodology, Investigation, Formal analysis, Data curation, Conceptualization. **Pedro Lucas Araújo do Nascimento:** Methodology, Investigation, Data curation. **Mazen Samara:** Writing – review & editing, Visualization, Validation. **Éric David:** Writing – review & editing, Supervision, Methodology, Funding acquisition, Conceptualization. **Guilhermino Jose Macedo Fechine:** Writing – review & editing, Visualization, Supervision, Conceptualization. **Maurício Alves da Motta Sobrinho:** Writing – review & editing, Supervision, Resources, Project administration, Funding acquisition, Conceptualization. **Nicole Raymonde Demarquette:** Writing – review & editing, Supervision, Resources, Project administration, Funding acquisition, Conceptualization.

Declaration of competing interest

The authors declare that they have no known competing financial interests or personal relationships that could have appeared to influence the work reported in this paper.

Acknowledgements

The authors would like to acknowledge Fundação de Amparo à Ciência e Tecnologia do Estado de Pernambuco (FACEPE) [IBPG-1816-3.06/19], Coordenação de Aperfeiçoamento de Pessoas de Nível Superior (CAPES) [Grant Number 88881.622794/2021-01, PrIntgrant 88887.310339/2018-00], Conselho Nacional de Desenvolvimento Científico e Tecnológico (CNPq) [Grant Number 311321/2023-2 and process 314093/2021-4], Fundação de Amparo à Pesquisa do Estado de São Paulo (FAPESP) [Process 2020/11496-0 and 2021/07858-7], Natural Sciences and Engineering Research Council of Canada (NSERC) [RGPIN-2024-03848] and Tier 1 Canadian Research Chair [CRC-2021-00489] for funding this work.

Appendix A. Supplementary data

Supplementary data to this article can be found online at <https://doi.org/10.1016/j.polymer.2025.128067>.

Data availability

Data will be made available on request.

References

- [1] S.O. Ilyin, S. V Kotomin, Effect of nanoparticles and their anisotropy on adhesion and strength in hybrid carbon-fiber-reinforced epoxy nanocomposites, *Journal of Composites Science* 7 (2023), <https://doi.org/10.3390/jcs7040147>.
- [2] S.M. Reduwan Billah, in: M.A. Jafar Mazumder, H. Sheardown, A. Al-Ahmed (Eds.), *Composites and Nanocomposites BT - Functional Polymers*, Springer International Publishing, Cham, 2019, pp. 1–67, https://doi.org/10.1007/978-3-319-92067-2_15-1.
- [3] A.K. Pathak, S.R. Dhakate, Validation of experimental results for graphene oxide-epoxy polymer nanocomposite through computational analysis, *J. Polym. Sci.* 59 (2021) 84–99, <https://doi.org/10.1002/pol.20200442>.
- [4] P.K. Balmuri, D.G.H. Samuel, U. Thumu, A review on mechanical properties of epoxy nanocomposites, *Mater Today Proc* 44 (2021) 346–355, <https://doi.org/10.1016/j.matpr.2020.09.742>.
- [5] X. Sun, C. Huang, L. Wang, L. Liang, Y. Cheng, W. Fei, Y. Li, Recent progress in graphene/polymer nanocomposites, *Adv. Mater.* 33 (2021) 2001105, <https://doi.org/10.1002/adma.202001105>.
- [6] S.M.N. Sultana, E. Helal, G. Gutiérrez, E. David, N. Moghimi, N.R. Demarquette, Effect of few-layer graphene on the properties of mixed polyolefin waste stream, *Crystals* 13 (2023) 1–14, <https://doi.org/10.3390/cryst13020358>.
- [7] Z.S.B. de Souza, G.M. Pinto, G. da C. Silva, N.R. Demarquette, G.J.M. Fechine, M.A. M. Sobrinho, Interface adjustment between poly(ethylene terephthalate) and graphene oxide in order to enhance mechanical and thermal properties of nanocomposites, *Polym. Eng. Sci.* 61 (2021) 1997–2011, <https://doi.org/10.1002/pen.25715>.
- [8] M. Martín-Gallego, R. Verdejo, M.A. Lopez-Manchado, M. Sangermano, Epoxy-Graphene UV-cured nanocomposites, *Polymer* 52 (2011) 4664–4669, <https://doi.org/10.1016/j.polymer.2011.08.039>.
- [9] A. Kausar, I. Ahmad, M.H. Eisa, M. Maaza, H. Khan, Manufacturing strategies for graphene derivative nanocomposites—current status and fruitions, *Nanomanufacturing* 3 (2023) 1–19, <https://doi.org/10.3390/nanomanufacturing3010001>.
- [10] S.J. Lee, S.J. Yoon, I.-Y. Jeon, Graphene/polymer nanocomposites: preparation, mechanical properties, and application, *Polymers* 14 (2022), <https://doi.org/10.3390/polym14214733>.
- [11] C. Ding, Z. Lin, Y. Li, Y. Fang, C. Tan, C. Wang, L. Lou, N. Liu, Z. Mao, J. Feng, Research and application of fast-curing anticorrosion inner coatings for vessels in an acid environment, *J Phys Conf Ser* 2539 (2023) 012015, <https://doi.org/10.1088/1742-6596/2539/1/012015>.
- [12] J.H. Shin, M.B. Yi, S.J. Lee, H.J. Kim, Rapid cure composites in electronics industry, rapid cure composites: materials, Processing and Manufacturing (2023) 179–212, <https://doi.org/10.1016/B978-0-323-98337-2.00015-8>.
- [13] F. Groh, E. Kappel, C. Hühne, W. Brymerski, Investigation of fast curing epoxy resins regarding process induced distortions of fibre reinforced composites, *Compos. Struct.* 207 (2019) 923–934, <https://doi.org/10.1016/j.compstruct.2018.09.003>.

- [14] N. Lorenz, M. Müller-Pabel, J. Gerritzen, J. Müller, B. Gröger, D. Schneider, K. Fischer, M. Gude, C. Hopmann, Characterization and modeling cure- and pressure-dependent thermo-mechanical and shrinkage behavior of fast curing epoxy resins, *Polym. Test.* 108 (2022) 107498, <https://doi.org/10.1016/j.POLYMERTESTING.2022.107498>.
- [15] M. Ghaffari, M. Ehsani, H.A. Khonakdar, G. Van Assche, H. Terryn, Evaluation of curing kinetic parameters of an epoxy/polyaminoamide/nano-glassflake system by non-isothermal differential scanning calorimetry, *Thermochim. Acta* 533 (2012) 10–15, <https://doi.org/10.1016/j.tca.2012.01.009>.
- [16] C. Verma, L.O. Olasunkanmi, E.D. Akpan, M.A. Quraishi, O. Dagdag, M. El Gouri, E.-S.M. Sherif, E.E. Ebenso, Epoxy resins as anticorrosive polymeric materials: a review, *React. Funct. Polym.* 156 (2020) 104741, <https://doi.org/10.1016/j.reactfunctpolym.2020.104741>.
- [17] S. Rehman, S. Akram, A. Kanelloupolous, A. Elmarakbi, P.G. Karagiannidis, Development of new graphene/epoxy nanocomposites and study of cure kinetics, thermal and mechanical properties, *Thermochim. Acta* 694 (2020) 178785, <https://doi.org/10.1016/J.TCA.2020.178785>.
- [18] X. Chen, W. Jiang, B. Hu, Z. Liang, Y. Zhang, J. Kang, Y. Cao, M. Xiang, Effects of graphene oxide size on curing kinetics of epoxy resin, *RSC Adv.* 11 (2021) 29215–29226, <https://doi.org/10.1039/D1RA05234A>.
- [19] M. Nonahal, M.R. Saeb, S. Hassan Jafari, H. Rastin, H.A. Khonakdar, F. Najafi, F. Simon, Design, preparation, and characterization of fast cure epoxy/amine-functionalized graphene oxide nanocomposites, *Polym. Compos.* 39 (2018) E2016–E2027, <https://doi.org/10.1002/pc.24415>.
- [20] L. Li, Z. Zeng, H. Zou, M. Liang, Curing characteristics of an epoxy resin in the presence of functional graphite oxide with amine-rich surface, *Thermochim. Acta* 614 (2015) 76–84, <https://doi.org/10.1016/j.tca.2015.06.006>.
- [21] S.H. Ryu, J.H. Sin, A.M. Shanmugaraj, Study on the effect of hexamethylene diamine functionalized graphene oxide on the curing kinetics of epoxy nanocomposites, *Eur. Polym. J.* 52 (2014) 88–97, <https://doi.org/10.1016/j.eurpolymj.2013.12.014>.
- [22] O. Vryonis, S.T.H. Virtanen, T. Andritsch, A.S. Vaughan, P.L. Lewin, Understanding the cross-linking reactions in highly oxidized graphene/epoxy nanocomposite systems, *J. Mater. Sci.* 54 (2019) 3035–3051, <https://doi.org/10.1007/s10853-018-3076-8>.
- [23] W. Li, T. Shang, W. Yang, H. Yang, S. Lin, X. Jia, Q. Cai, X. Yang, Effectively exerting the reinforcement of dopamine reduced graphene oxide on epoxy-based composites via strengthened interfacial bonding, *ACS Appl. Mater. Interfaces* 8 (2016) 13037–13050, <https://doi.org/10.1021/acsami.6b02496>.
- [24] J.C. Domínguez, Rheology and curing process of thermosets. Thermosets: Structure, Properties, and Applications, second ed., 2018, <https://doi.org/10.1016/B978-0-08-101021-1.00004-6>, 115–146.
- [25] L.S. Cividanes, E.A.N. Simonetti, M.B. Moraes, F.W. Fernandes, G.P. Thim, Influence of carbon nanotubes on epoxy resin cure reaction using different techniques: a comprehensive review, *Polym. Eng. Sci.* 54 (2014) 2461–2469, <https://doi.org/10.1002/pen.23775>.
- [26] J. Trinidad, B.M. Amoli, W. Zhang, R. Pal, B. Zhao, Effect of SDS decoration of graphene on the rheological and electrical properties of graphene-filled epoxy/Ag composites, *J. Mater. Sci. Mater. Electron.* 27 (2016) 12955–12963, <https://doi.org/10.1007/s10854-016-5434-0>.
- [27] W.S. Hummers, R.E. Offeman, Preparation of graphitic oxide, *J. Am. Chem. Soc.* 80 (1958) 1339, <https://doi.org/10.1021/ja01539a017>.
- [28] C.M.B. Araujo, R.B. Assis Filho, A.M.S. Baptistella, G.F.O. Nascimento, G.R. B. Costa, M.N. Carvalho, M.G. Ghislandi, M.A. da Motta Sobrinho, Systematic study of graphene oxide production using factorial design techniques and its application to the adsorptive removal of methylene blue dye in aqueous medium, *Mater. Res. Express* 5 (2018) 065042, <https://doi.org/10.1088/2053-1591/aacb51>.
- [29] T.J.M. Fraga, L.E.M. de Lima, Z.S.B. de Souza, M.N. Carvalho, E.M.P.L. Freire, M. G. Ghislandi, M.A. da Motta, Amino-Fe₃O₄-functionalized graphene oxide as a novel adsorbent of Methylene Blue: kinetics, equilibrium, and recyclability aspects, *Environ. Sci. Pollut. Control Ser.* (2018), <https://doi.org/10.1007/s11356-018-3139-z>.
- [30] J. Lange, N. Altmann, C.T. Kelly, P.J. Halley, Understanding vitrification during cure of epoxy resins using dynamic scanning calorimetry and rheological techniques, *Polymer* 41 (2000) 5949–5955, [https://doi.org/10.1016/S0032-3861\(99\)00758-2](https://doi.org/10.1016/S0032-3861(99)00758-2).
- [31] A. Surendran, J. Pionteck, R. Vogel, N. Kalarikkal, G. V G, S. Thomas, Effect of organically modified clay on the morphology, rheology and viscoelasticity of epoxy–thermoplastic nanocomposites, *Polym. Test.* 70 (2018) 18–29, <https://doi.org/10.1016/j.polymertesting.2018.06.023>.
- [32] S. Ganguli, D. Dean, K. Jordan, G. Price, R. Vaia, Chemorheology of cyanate ester—organically layered silicate nanocomposites, *Polymer* 44 (2003) 6901–6911, <https://doi.org/10.1016/J.POLYMER.2003.08.031>.
- [33] H.H. Winter, F. Chambon, Analysis of linear viscoelasticity of a crosslinking polymer at the gel point, *J Rheol (N Y N Y)* 30 (1986) 367–382, <https://doi.org/10.1122/1.549853>.
- [34] E.E. Holly, S.K. Venkataraman, F. Chambon, H. Henning Winter, Fourier transform mechanical spectroscopy of viscoelastic materials with transient structure, *J Nonnewton Fluid Mech* 27 (1988) 17–26, [https://doi.org/10.1016/0377-0257\(88\)80002-8](https://doi.org/10.1016/0377-0257(88)80002-8).
- [35] N. Lorenz, W.E. Dyer, B. Kumru, Thermo-rheological and kinetic characterization and modeling of an epoxy vitrimer based on polyimine exchange, *Soft Matter* 20 (2024) 6289–6301, <https://doi.org/10.1039/D4SM00724G>.
- [36] M.L. Auad, S.R. Nutt, P.M. Stefani, M.I. Aranguren, Rheological study of the curing kinetics of epoxy–phenol novolac resin, *J. Appl. Polym. Sci.* 102 (2006) 4430–4439, <https://doi.org/10.1002/app.24674>.
- [37] F. Wu, X. Zhou, X. Yu, Reaction mechanism, cure behavior and properties of a multifunctional epoxy resin, TGDDM, with latent curing agent dicyandiamide, *RSC Adv.* 8 (2018) 8248–8258, <https://doi.org/10.1039/C7RA13233F>.
- [38] D.A. Janzen, M.F. Diniz, J.B. Azevedo, J.R.A. Pinto, N.B. Sanches, R.D.C.L. Dutra, Qualitative and quantitative evaluation of epoxy systems by fourier transform infrared spectroscopy and the flexibilizing effect of mercaptans, *An. Acad. Bras. Cienc.* 93 (2021) 1–20, <https://doi.org/10.1590/0001-3765202120200799>.
- [39] J. Ederer, P. Janoš, P. Ecorchard, J. Tolasz, V. Stengl, H. Beneš, M. Perchacz, O. Pop-Georgievski, Determination of amino groups on functionalized graphene oxide for polyurethane nanomaterials: XPS quantitation vs. functional speciation, *RSC Adv.* 7 (2017) 12464–12473, <https://doi.org/10.1039/c6ra28745j>.
- [40] K. Dave, K.H. Park, M. Dhayal, Two-step process for programmable removal of oxygen functionalities of graphene oxide: functional, structural and electrical characteristics, *RSC Adv.* 5 (2015) 95657–95665, <https://doi.org/10.1039/C5RA18880F>.
- [41] A.I. Pruna, A. Barjola, A.C. Cárcel, B. Alonso, E. Giménez, Effect of varying amine functionalities on CO₂ capture of carboxylated graphene oxide-based cryogels, *Nanomaterials* 10 (2020), <https://doi.org/10.3390/nano10081446>.
- [42] B. Meschi Amoli, J. Trinidad, G. Rivers, S. Sy, P. Russo, A. Yu, N.Y. Zhou, B. Zhao, SDS-stabilized graphene nanosheets for highly electrically conductive adhesives, *Carbon N Y* 91 (2015) 188–199, <https://doi.org/10.1016/j.carbon.2015.04.039>.
- [43] C.F.P. De Oliveira, P.A.R. Muñoz, M.C.C. Santos, G.S. Medeiros, A. Simionato, D. A. Nagaoka, E.A.T. De Souza, S.H. Domingues, G.J.M. Fecchine, Tuning of surface properties of poly (vinyl alcohol)/graphene oxide nanocomposites, *Polym. Compos.* 40 (2019) E312–E320, <https://doi.org/10.1002/pc.24659>.
- [44] A.M. Shanmugaraj, J.H. Yoon, W.J. Yang, S.H. Ryu, Synthesis, characterization, and surface wettability properties of amine functionalized graphene oxide films with varying amine chain lengths, *J. Colloid Interface Sci.* 401 (2013) 148–154, <https://doi.org/10.1016/j.jcis.2013.02.054>.
- [45] M. Nonahal, M.R. Saeb, S. Hassan Jafari, H. Rastin, H.A. Khonakdar, F. Najafi, F. Simon, Design, preparation, and characterization of fast cure epoxy/amine-functionalized graphene oxide nanocomposites, *Polym. Compos.* 39 (2018) E2016–E2027, <https://doi.org/10.1002/pc.24415>.
- [46] S. Ganguli, D. Dean, K. Jordan, G. Price, R. Vaia, Chemorheology of cyanate ester—organically layered silicate nanocomposites, *Polymer* 44 (2003) 6901–6911, <https://doi.org/10.1016/J.POLYMER.2003.08.031>.
- [47] M.G. González, J.C. Cabanelas, J. Baselga, in: T. Theophanides (Ed.), Applications of FTIR on Epoxy Resins - Identification, Monitoring the Curing Process, Phase Separation and Water Uptake, 2012, <https://doi.org/10.5772/36323>, IntechOpen, Rijeka Ch. 13.
- [48] D.L. Pavia, G.M. Lampman, G.S. Kriz, J.A. Vyvyan, *Introduction to Spectroscopy*, 4th, Cengage Learning, 2008.
- [49] B.M.V. Romão, M.F. Diniz, M.F.P. Azevedo, V.L. Lourenço, L.C. Pardini, R.C. L. Dutra, F. Burel, Characterization of the curing agents used in epoxy resins with TG/FT-IR technique, *Polimeros* 16 (2006) 94–98, <https://doi.org/10.1590/S0104-14282006000200007>.
- [50] N. El-Thaher, T. Mekonnen, P. Mussone, D. Bressler, P. Choi, Nonisothermal DSC study of epoxy resins cured with hydrolyzed specified risk material, *Ind. Eng. Chem. Res.* 52 (2013) 8189–8199, <https://doi.org/10.1021/ie400803d>.
- [51] D.G.D. Galpaya, J.F.S. Fernando, L. Rintoul, N. Motta, E.R. Waclawik, C. Yan, G. A. George, The effect of graphene oxide and its oxidized debris on the cure chemistry and interphase structure of epoxy nanocomposites, *Polymer* 71 (2015) 122–134, <https://doi.org/10.1016/J.POLYMER.2015.06.054>.
- [52] F.V. Ferreira, F.S. Brito, W. Franceschi, E.A.N. Simonetti, L.S. Cividanes, M. Chipara, K. Lozano, Functionalized graphene oxide as reinforcement in epoxy based nanocomposites, *Surface. Interfac.* 10 (2018) 100–109, <https://doi.org/10.1016/J.SURFIN.2017.12.004>.
- [53] Y. Wei, X. Hu, Q. Jiang, Z. Sun, P. Wang, Y. Qiu, W. Liu, Influence of graphene oxide with different oxidation levels on the properties of epoxy composites, *Compos. Sci. Technol.* 161 (2018) 74–84, <https://doi.org/10.1016/J.COMPOSITECH.2018.04.007>.
- [54] A. Surnova, D. Balkaev, D. Musin, R. Amirov, A.M. Dimiev, Fully exfoliated graphene oxide accelerates epoxy resin curing, and results in dramatic improvement of the polymer mechanical properties, *Compos. B Eng.* 162 (2019) 685–691, <https://doi.org/10.1016/J.COMPOSITESB.2019.01.020>.
- [55] M. Naeem, H.C. Kuan, A. Michelmore, Q. Meng, A. Qiu, M. Aakyiir, D. Losic, S. Zhu, J. Ma, A new method for preparation of functionalized graphene and its epoxy nanocomposites, *Compos. B Eng.* 196 (2020) 108096, <https://doi.org/10.1016/J.COMPOSITESB.2020.108096>.
- [56] L. Shen, X. Zhang, Y. Lei, M. Liang, Y. Chen, W. Chen, H. Zou, Efficient reinforcement of epoxy resin with amine-rich rigid short-chain grafted graphene oxide, *Polym. Compos.* 42 (2021) 4775–4785, <https://doi.org/10.1002/PC.26186>.
- [57] F.V. Ferreira, F.S. Brito, W. Franceschi, E.A.N. Simonetti, L.S. Cividanes, M. Chipara, K. Lozano, Functionalized graphene oxide as reinforcement in epoxy based nanocomposites, *Surface. Interfac.* 10 (2018) 100–109, <https://doi.org/10.1016/J.SURFIN.2017.12.004>.
- [58] C. Zeng, S. Lu, L. Song, X. Xiao, J. Gao, J. Pan, Z. He, J. Yu, Enhanced thermal properties in a hybrid graphene–alumina filler for epoxy composites, *RSC Adv.* 5 (2015) 35773–35782, <https://doi.org/10.1039/C5RA01967B>.